

Experimental Evidence Supported by Simulations of a Very High H₂ Diffusion in Metal Organic Framework Materials

F. Salles,¹ H. Jobic,² G. Maurin,^{1,*} M.M. Koza,³ P.L. Llewellyn,⁴ T. Devic,⁵ C. Serre,⁵ and G. Férey⁵

¹*Institut Charles Gerhardt Montpellier, UMR CNRS 5253, UM2, ENSCM, Place E. Bataillon, 34095 Montpellier cedex 05 France*

²*Institut de Recherches sur la Catalyse et l'Environnement de LYON, CNRS, Université de Lyon,
2. Av. A. Einstein, 69626 Villeurbanne, France*

³*Institut Laue Langevin, BP 156, 38042 Grenoble, France*

⁴*Laboratoire Chimie Provence, Universités d'Aix-Marseille I,II et III - CNRS, UMR 6264, Centre de Saint Jérôme,
13397 Marseille, France*

⁵*Institut Lavoisier, UMR CNRS 8180, Université de Versailles Saint-Quentin-en-Yvelines, 78035 Versailles Cedex, France*

(Received 17 March 2008; published 17 June 2008)

Quasielastic neutron scattering measurements are combined with molecular dynamics simulations to extract the self-diffusion coefficient of hydrogen in the metal organic frameworks MIL-47(V) and MIL-53(Cr). We find that the diffusivity of hydrogen at low loading is about 2 orders of magnitude higher than in zeolites. Such a high mobility has never been experimentally observed before in any nanoporous materials, although it was predicted in carbon nanotubes. Either 1D or 3D diffusion mechanisms are elucidated depending on the chemical features of the MIL framework.

DOI: [10.1103/PhysRevLett.100.245901](https://doi.org/10.1103/PhysRevLett.100.245901)

PACS numbers: 66.30.je, 25.40.Dn, 31.15.xv, 67.63.Cd

In the future energy economy, hydrogen is proposed as an important potential energy carrier. However, one of the major issues for portable applications of this energy vector relies on its economic and safe pressure storage under the conditions of transport. Research efforts have been mostly focused on the development of porous materials, including single-walled carbon nanotubes, zeolites, and activated carbons with the ability to adsorb and store hydrogen under economically viable conditions. The U.S. Department of Energy (DOE) has set the target for hydrogen storage at 6.0 wt % in the temperature range 253–353 K in 2010 [1]. Metal-organic frameworks (MOFs), which combine both an inorganic node containing metal centers and an organic linker moiety (carboxylates, phosphonates or imidazoles), have been also intensively investigated during the last few years for that purpose [2–5]. They are particularly promising as they combine a low framework density, high sorption capacities up to 7.5 wt % at 77 K [4] and low regeneration costs. More recently, it has been predicted that their adsorption capacities can be strongly enhanced by the introduction of lithium cations which lead to a negatively charged framework [6]. However, besides the required high adsorption capacity under various conditions, a fast hydrogen diffusion rate in these materials is essential for the development of transport kinetics based devices. Indeed, in order to evaluate the potential applicability of these hybrid porous systems for the hydrogen fuel economy, one has to gain a more precise understanding on the molecular transport properties of hydrogen within the micropores of these materials. Skoulidas and Sholl were the first to report a theoretical investigation of both self- and transport diffusivity of H₂ in MOF-5 [7]. This study was followed by those of Yang *et al.* [8], and Liu *et al.* [9] who predicted the self-diffusivity behavior of H₂ in IRMOFs and new Zn based MOF materials. However, no

experimental data are yet available in the literature to support these simulations. Here, we report the first experimental exploration of the self-diffusivity D_s , of hydrogen in MOF-type materials by means of quasielastic neutron scattering (QENS) measurements. Up to now, only pulsed field gradient NMR diffusion measurements have been reported on hydrocarbons in MOF-5 [10]. More recently, interference microscopy has been used to study the intracrystalline diffusion of methanol in MOF manganese formate [11]. The QENS technique has proved to be very powerful to extract the loading dependence of the diffusivities for a wide range of adsorbates, including hydrogen, in zeolites [12,13]. Combining this experimental technique with molecular simulation has been successful to characterize the diffusion mechanism of various adsorbates in nanoporous materials [13]. Here, the conclusions drawn from our QENS investigations are thus supported by Molecular Dynamics simulations. The selected MOFs are the MIL-53(Cr) and MIL-47(V) systems which belong to the MIL (Materials of the Institut Lavoisier) series of hybrid porous materials, synthesized by the group of Férey. The MIL-53(Cr) and its isostructural form MIL-47(V), are built up from infinite chains of corner-sharing Cr³⁺O₄(OH)₂ or V⁴⁺O₆ octahedra interconnected by 1,4-benzenedicarboxylate groups [14,15]. This 3D MOF contains 1D diamond shaped channels with pores of nanometer dimensions. One notes that the MIL-53(Cr) exhibits hydroxyl groups located at the metal-oxygen-metal links (μ_2 -OH groups) which open up the possibility of additional preferential adsorption sites and thus different adsorption or diffusion mechanisms to that of MIL-47(V) where these specific groups are absent.

QENS measurements were performed on the time-of-flight spectrometer IN6, at the Institut Laue Langevin, Grenoble, France. Because of the large incoherent cross

section of hydrogen, QENS monitors the self-diffusion of the adsorbate [12,13]. To reduce the signal from the MOFs, the framework was deuterated. An incident neutron energy of 3.12 meV (5.1 Å) was applied, leading to a wave vector transfer range, Q , from 0.24 to 2.1 Å⁻¹. Different detectors were grouped for reasonable counting statistics and spectra displaying Bragg peaks of the MIL frameworks were suppressed in the data. Time-of-flight spectra were then converted to energy spectra. The elastic line could be fitted by a Gaussian function, whose half-width at half-maximum (HWHM) varies from 40 μeV at small Q to 50 μeV at large Q . Four different H₂ loadings, determined by volumetry during the QENS experiment, were investigated for both MIL-47(V) and MIL-53(Cr) systems. For the third loading, runs were performed at three different temperatures to obtain the activation energy of the diffusion process. Some of the resulting QENS spectra recorded at 77 K are shown in Fig. 1. The measured intensities are presented in terms of the dynamical structure factor, $S(Q, \omega)$, where Q and $\hbar\omega$ are the wave vector and energy transfers, re-

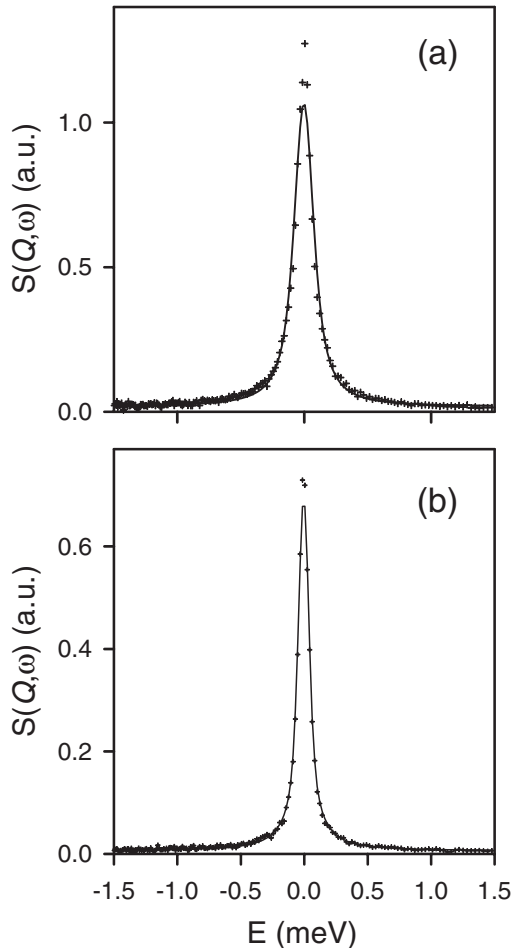


FIG. 1. Comparison between experimental and fitted QENS spectra obtained for H₂ (a) in MIL-47 (V) for 3.4 molecules per u.c., on average; the solid line corresponds to a 3D diffusion; (b) in MIL-53 (Cr) for 3.5 molecules per unit cell (u.c.), the solid line is computed for a 1D diffusion ($T = 77$ K, $Q = 0.27$ Å⁻¹).

spectively. The spectra were first fitted individually with a Lorentzian function, corresponding to the diffusion motion, convoluted with the instrumental resolution. It was found that a 3D diffusion model for H₂ reproduces well the QENS spectra for MIL-47(V) (Fig. 1). In contrast, for MIL-53(Cr), a unidimensional diffusion model is required to fit better the experimental spectra (Fig. 1). This observation is consistent with previous findings which showed that the peak shape is more elongated for 1D than for 3D diffusion, because a powder average of the 1D dynamical structure factor has to be made [16]. The HWHM of the dynamical structure factor is reported in Fig. 2, at small Q values, for various H₂ loadings in MIL-53(Cr) at 77 K. One can extract from the QENS data not only D_s , but also, using jump diffusion models, information on the elementary steps of the diffusion process. In MIL-53(Cr), all spectra could be fitted simultaneously with a 1D jump diffusion model, having a fixed jump length (Fig. 2). The shift of the maximum of the curve to lower Q values, when the H₂ concentration decreases, indicates an increase of the jump length. At the largest loading, the jump length is 7.5 Å, which is similar to the distance between two consecutive μ_2 -OH groups situated along the tunnel (y axis), separated by 6.8 Å. This jump length increases up to 12.3 Å for the lowest loading, emphasizing that a lower probability of H₂/H₂ collisions when the loading decreases leads to H₂ displacements over longer distances. In MIL-47(V), a 3D jump diffusion model with a distribution of jump lengths allowed to fit simultaneously all spectra; the mean jump lengths also decrease when the loading increases, the values being 4.3 to 22 Å for the highest and lowest H₂ concentrations, respectively. The mean jump length observed at lowest loading is much higher than those found for MIL-53(Cr), which clearly shows that the presence of the μ_2 -OH groups restricts the magnitude of the maximum H₂ displacements.

Figure 3 reports the resulting D_s for both MIL-47(V) and MIL-53(Cr) at 77 K, within an error bar of 20%. It has to be mentioned that the self-diffusivity values for MIL-53(Cr) are orientationally averaged: $D_s = D_{1D}/3$. In both MILs, as previously observed in MOF-5 [9], D_s decreases as the loading increases due mainly to steric interactions, with the characteristic $d(\text{H}_2\text{-H}_2)$ distance between adsorbate molecules becoming significantly shorter. Further, MIL-47(V) exhibits a significantly higher diffusivity than MIL-53(Cr) in the whole range of investigated loading (Fig. 3), which is consistent with a lower activation energy for MIL-47(V), i.e., 0.6 kJ · mol⁻¹ vs 1.6 kJ · mol⁻¹. These results can be explained by the presence of the μ_2 -OH groups in MIL-53(Cr) which act as attractive sites and steric barriers for H₂, thus leading to a slower diffusion process.

Moreover, a high H₂ mobility is observed for both MILs as indicated by the large D_s value obtained at low loading (Fig. 3). Indeed, an extrapolation of D_s leads to a minimal value of 10⁻⁶ m² · s⁻¹ at 77 K for MIL-47(V). Further, from the experimental activation energy, it is possible to estimate a D_s value of 2 × 10⁻⁶ m² · s⁻¹ at 300 K in this

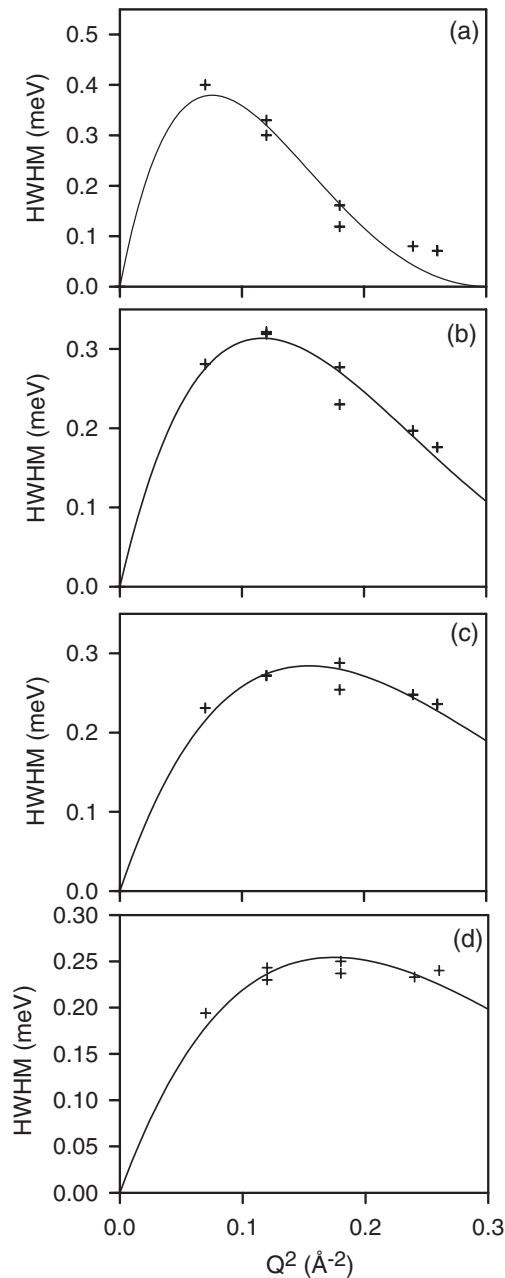


FIG. 2. Half-width at half-maximum of the dynamical structure factor vs Q^2 for H_2 in MIL-53 (Cr) at different loadings (a) 0.71 H_2 /u.c., (b) 1.53 H_2 /u.c., (c) 2.50 H_2 /u.c., (d) 3.50 H_2 /u.c. ($T = 77$ K). The crosses (+) were obtained from individual fits of the spectra, the curves with simultaneous 1D fits with all spectra.

MOF, which is much higher than those observed in liquid hydrogen ($\sim 10^{-8} \text{ m}^2 \cdot \text{s}^{-1}$) [17] and computed in other MOFs ($\sim 2 \times 10^{-7} \text{ m}^2 \cdot \text{s}^{-1}$) [7,9] for the same range of temperature. This diffusivity is also about 2 orders of magnitude higher than in zeolites (from 10^{-8} to $10^{-10} \text{ m}^2 \cdot \text{s}^{-1}$ at room temperature) [18]. This behavior is reminiscent of the very fast H_2 diffusivity predicted in single-walled carbon nanotubes although our D_s value remains somewhat lower [19,20].

The high change of gradient observed for D_s at low loading (Fig. 3) has never been experimentally evidenced in any nanoporous material, although it was previously predicted for both H_2 and CH_4 in single-walled carbon nanotubes [19,20]; this unusual behavior has neither been simulated for other MOFs, where only an almost linear increase of D_s was obtained when the loading decreases [7,9]. It can be explained by a smooth H_2 /MOF framework potential energy surface as argued previously in the case of carbon nanotubes [19].

To more deeply understand the diffusion mechanism of H_2 at the microscopic scale, molecular dynamics simulations (MD) were performed for both MIL materials at 77 K in the NVT ensemble using the Evans isokinetic thermostat [21]. Tests calculations using NVE-MD trajectories, generated equivalent diffusivities within an error bar less than 5%. A simulation box corresponding to 16 unit cells of both MILs was considered. These simulations were performed for different loadings consistent with the experimental ones, each for $2 \cdot 10^6$ steps (i.e. 2 ns) with a time step of 1 fs, following 50 000 steps of equilibration. In order to evaluate the activation energies corresponding to the self-diffusion process, additional simulations were performed for 3 H_2 molecules per unit cell in a range of temperature between 50 and 150 K. The potential parameters for describing H_2 were extracted from the literature [22]. For the interactions between H_2 and both organic and inorganic moieties, the parameters of H_2 were initially combined with that taken from the widely used UFF forcefield [23], using Lorentz-Berthelot mixing rules. These adsorbate/adsorbent potential parameters were slightly adjusted by about 5% to reproduce better the experimental isotherms and enthalpies of adsorption in both MIL-53(Cr) and MIL-47(V).

From the mean square displacement (MSD) curves, it was thus possible to extract the self-diffusion coefficient D_s according to Einstein's relation, as a function of loading. As depicted in Fig. 3, the simulated data are in good agreement with those measured by QENS for both MILs, although the simulations fail to match the sharp increase of

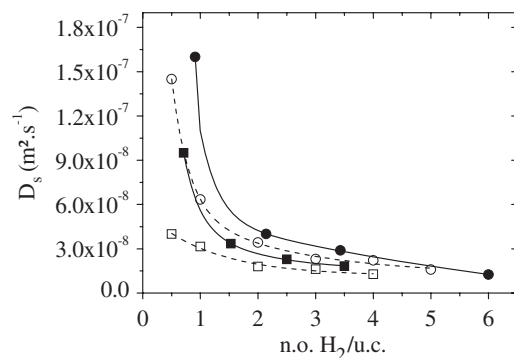


FIG. 3. Self-diffusivities (D_s) for both MIL-47 (V) (○) and MIL-53(Cr) (□) as a function of the loading at 77 K: QENS (full symbols), MD (empty symbols).

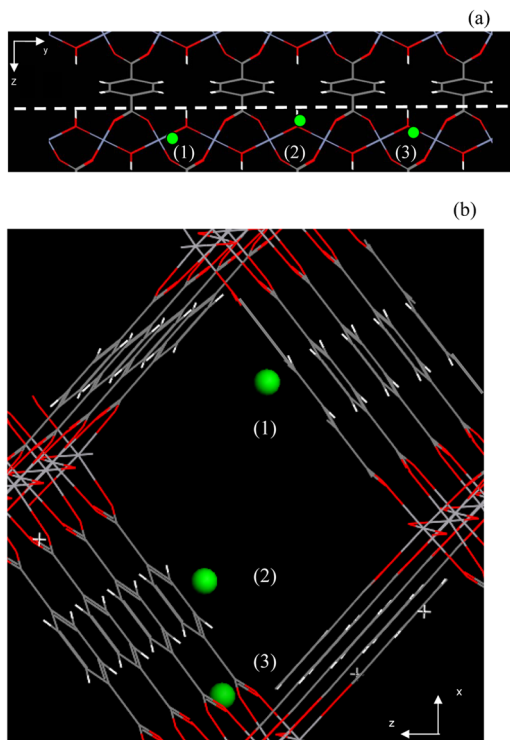


FIG. 4 (color online). Typical illustration of the diffusion mechanism of H_2 in MIL-53(Cr) (a) and MIL-47(V) (b). For MIL-53(Cr), the snapshots from 1 to 3 correspond to the jump sequence of H_2 along the tunnel observed during the MD runs (the diffusion lengths between 1-2 and 2-3 correspond to about 6.8 Å and the times for each interval are 7.3 and 6.8 ps, respectively). For MIL-47(V), the H_2 is randomly displaced within the pore as attested by its location in 1, 2, and 3 obtained at different times of the MD runs. The direction of the tunnel is along the y axis.

D_s at low loading for MIL-53(Cr). The faster diffusion process in MIL-47(V) is also reproduced by our simulations, with a corresponding activation energy ($0.6 \text{ kJ} \cdot \text{mol}^{-1}$), lower than the one calculated for MIL-53(Cr) ($1.3 \text{ kJ} \cdot \text{mol}^{-1}$). Both simulated values compare well with the above mentioned experimental activation energies. Further, in order to get a raw estimation of D_s in the limit of dilute loading, MD simulations were performed at 77 and 300 K for MIL-47(V) switching off the H_2/H_2 interactions. In that way, 16 H_2 molecules in a larger simulation box containing 32 unit cells and longer MD runs (up to 5 ns) were considered to ensure good statistics. The resulting D_s values are $1.9 \times 10^{-7} \text{ m}^2 \cdot \text{s}^{-1}$ and $4.0 \times 10^{-7} \text{ m}^2 \cdot \text{s}^{-1}$ at 77 and 300 K, respectively, and as already observed in Fig. 3 at 77 K, they underestimate the experimental values.

Further, as illustrated in Fig. 4(a), it is clear that the diffusion of H_2 in MIL-53(Cr) is mainly governed by the interaction between H_2 and the hydroxyl groups, leading to a 1D diffusion along the tunnel via a jump sequence

involving these μ_2 -OH groups. This microscopic mechanism supports both the use of a 1D diffusion model to fit the QENS spectra (Fig. 1), and the evolution of the HWHM of the dynamical structure factor when the hydrogen loading decreases (Fig. 2). In contrast, in MIL-47(V), simulations show a 3-dimensional diffusion process with random motions of H_2 within the pore of the material [Fig. 4(b)], which is consistent with the previous experimental findings.

Our experimental QENS measurements thus provide for the first time a clear evidence of a high mobility of a light gas in nanoporous materials. Coupled with molecular simulation, it is possible to distinguish a 1D or 3D microscopic diffusion mechanisms depending on the chemical features of the MOF surface.

This work was supported by the French program ANR CO_2 “NoMAC” (ANR-06- CO_2 -008).

*Corresponding author.

gmaurin@lpmc.univ-montp2.fr

- [1] S. Satyapal *et al.*, *Catalysis Today* **120**, 246 (2007).
- [2] G. Férey, *Chem. Soc. Rev.* **37**, 191 (2008).
- [3] N.L.Rosi *et al.*, *Science* **300**, 1127 (2003).
- [4] M. Latroche *et al.*, *Angew. Chem., Int. Ed.* **45**, 8227 (2006).
- [5] B. Panella *et al.*, *Angew. Chem., Int. Ed.* **47**, 2138 (2008).
- [6] S. Soo Han, W.-Q. Deng, and W. A. Goddard, III, *Angew. Chem., Int. Ed.* **46**, 6289 (2007).
- [7] A.I. Skoulidas and D. S. Sholl, *J. Phys. Chem. B* **109**, 15760 (2005).
- [8] Q. Yang and C. Zhong, *J. Phys. Chem. B* **109**, 11 862 (2005).
- [9] J. Liu *et al.*, *J. Phys. Chem. C* **112**, 2911 (2008).
- [10] F. Stallmach *et al.*, *Angew. Chem., Int. Ed.* **45**, 2123 (2006).
- [11] P. V. Kortunov *et al.*, *J. Am. Chem. Soc.* **129**, 8041 (2007).
- [12] H. Jovic, J. Kärger, and M. Bée, *Phys. Rev. Lett.* **82**, 4260 (1999).
- [13] H. Jovic and D. N. Theodorou, *Microporous Mesoporous Mater.* **102**, 21 (2007).
- [14] C. Serre *et al.*, *J. Am. Chem. Soc.* **124**, 13 519 (2002).
- [15] K. Barthelet *et al.*, *Angew. Chem., Int. Ed.* **41**, 281 (2002).
- [16] H. Jovic *et al.*, *J. Phys. Chem. B* **101**, 5834 (1997).
- [17] G. Cini-Castagnoli, A. Giardini-Guidoni, and F. P. Ricci, *Phys. Rev.* **123**, 404 (1961).
- [18] N. K. Bär *et al.*, *Magn. Reson. Chem.* **37**, S79 (1999).
- [19] A.I. Skoulidas *et al.*, *Phys. Rev. Lett.* **89**, 185901 (2002).
- [20] G. Garberoglio and R. Vallauri, *Phys. Lett. A* **316**, 407 (2003).
- [21] D. Frenkel and B. Smit, *Understanding Molecular Simulation* (Academic, San Diego, CA, 1996).
- [22] H. Frost, T. Düren, and R. Q. Snurr, *J. Phys. Chem. B* **110**, 9565 (2006).
- [23] A. K. Rappé *et al.*, *J. Am. Chem. Soc.* **114**, 10024 (1992).